Control and Optimization in Applied Mathematics (COAM)
Vol. 7, No. 2, Summer-Autumn 2022 (77-98), ©2016 Payame Noor University, Iran

DOI. 10.30473/coam.2022.62261.1207 (Cited this article)

Research Article

Using the Integral Operational Matrix of B-Spline Functions to Solve Fractional Optimal Control Problems

Yousef Edrisi-Tabriz[*]

Department of Mathematics, Payame Noor University (PNU), P.O. BOX 19395-4697, Tehran, Iran.

Received: June 11, 2022 ; **Accepted:** November 17, 2022 .

Abstract. In this paper, we present a numerical method for solving the fractional optimal control problems in which fractional integral operational matrices of basic B-spline functions are used. In the proposed method, we use the Riemann-Liouville fractional integral. With the help of the operational matrix of the fractional integral and the collocation method, we transform the fractional optimal control problem into a nonlinear programming problem and then solve it with an appropriate optimization algorithm. Compared to similar numerical techniques, our method has better accuracy and efficiency, and also it is easy to use. To provide a clear view of the applicability and efficiency of our numerical method, several illustrative examples are presented.

Keywords. Fractional optimal control problem, Riemann-Leiville fractional integral, Operational matrix, B-Spline function, Collocation method.

MSC. 49N10; 65D07; 65R10; 65L60.

[*] Corresponding author
yousef_edrisi@pnu.ac.ir
http://mathco.journals.pnu.ac.ir

1 Introduction

Currently, one of the most widely used parts of applied mathematics belongs to fractional calculus. In recent years, this field has become an emerging position for science and engineering researchers with a wide range of applications. The range of applications of fractional calculus is increasing rapidly, including in pharmacokinetics [32], hyperchaotic system [30], radar-guided missile [36], quantum mechanics [20], stochastic programming [7], control theory [23], and image processing [1]. Numerical methods for solving fractional optimal control problems (FOCPs), on the other hand, have received much attention in recent years due to their ease of use and flexibility. Increasing the accuracy of these methods improves the results in practical applications, so the development of more accurate methods is of interest to researchers. Direct and indirect methods are the two main approaches in solving optimal control problems (OCPs) and more recently FOCPs [26]. In the current paper, we use a direct method to solve such problems. To use the direct method, a basic polynomial is needed to discretize FOCP. Various methods are developed with different polynomials such as Legendre [21], Jacobi [9], Bernstein [24], Boubaker [25] and Taylor polynomials [39]. Some other works in solving FOCPs that have been done recently and are of high accuracy are [3, 4, 15, 31, 37, 38]. Here, we use linear B-spline functions as basic polynomials [17]. Spline and B-spline polynomials were first introduced by Schoenberg in 1946 in his landmark paper. In this article, he states the theoretical foundations for this issue [28, 29, 34]. Due to the desirable properties of polynomial splines, they play a significant role in numerical analysis and approximation theory. Lakestani et al. [18] constructed the operational matrix of fractional derivatives using B-spline functions and solved fractional differential equations with the help of this matrix. This matrix was then used to solve various problems, including the problem of OCP in [11].

In numerical methods, sometimes an operational matrix of derivation [10, 11], and sometimes an operational matrix of integration [6, 12], is used. We choose the operational matrix for Riemann-Liouville integration. We represent this matrix with the equation.

$$I^{\alpha}\Phi_M(t) \approx \mathcal{I}^{\alpha}\Phi_M(t),$$

where I^{α} is the Riemann-Liouville integral operator of order α, $\mathcal{I}^{\alpha}$ is the operational matrix of fractional integration and the elements of $\Phi_M(t)$ are B-spline basis functions. We utilize this matrix to transform FOCPs into a nonlinear programming one and then solve it by suitable algorithms. In this paper, the operational matrix of the Riemann-Liouville fractional integral of B-spline functions are rewritten with the help of Laplace transforms, then using this matrix and in the form of a new numerical method, the fractional optimal control problem is solved. The results of the new numerical method are compared with the results of the numerical methods described in [6, 13, 15, 21, 35].

The paper is organized as follows. First of all, in Section 2, some preliminaries of fractional calculus and some necessary definitions of linear B-spline functions are briefly reviewed. Details on the construction of the operational matrix of fractional integration are reported in Section 3. The structure of the fractional optimal control problems is stated in Section 4. The new numerical method is presented in Section 5. In Section 6, the convergence of the proposed method is considered. In Section 7, we apply our numerical method to solve four examples. Finally, Section 8 completes this paper with a brief conclusion.

2 Introductory Definitions

2.1 The Caputo Fractional Derivative and the Riemann-Liouville Integral Operator

Definition 1. The Caputo fractional-order derivative is defined by [8]

$$D^{\alpha}\mathbf{x}(t) = \frac{1}{\Gamma(n-\alpha)}\int_0^t \frac{\mathbf{x}^{(n)}(\tau)}{(t-\tau)^{\alpha+1-n}}\,\mathrm{d}\tau, \;\; n-1<\alpha\leq n, \;\; n\in\mathbb{N}, \tag{1}$$

where $\alpha > 0$ is the order of the derivative and n is the smallest integer not less than α.

Definition 2. The Riemann-Liouville fractional integral operator of order α is defined by [8]

$$I^{\alpha}\mathbf{x}(\mathbf{t}) = \begin{cases} \dfrac{1}{\Gamma(\alpha)}\displaystyle\int_0^t \frac{x(\tau)}{(t-\tau)^{1-\alpha}}\,\mathrm{d}\tau = \frac{1}{\Gamma(\alpha)}t^{q-1} * \mathbf{x}(t), & \alpha > 0, \\ \mathbf{x}(t), & \alpha = 0, \end{cases} \tag{2}$$

where $*$ indicates the convolution product.

The relationship between the Caputo derivative and Riemann-Liouville integral is given in the following equation [8]

$$I^{\alpha}(D^{\alpha}\mathbf{y}(t)) = \mathbf{y}(t) - \sum_{k=0}^{n-1}\frac{t^k}{k!}\mathbf{y}^{(k)}(0), \tag{3}$$

where $n-1<\alpha\leqslant n$ and $\mathbf{y}^{(k)}(0)$ are the k-th order derivative of $\mathbf{y}(t)$ at $t=0$.

2.2 Linear B-Spline Functions

A spline function of order n complies with a piecewise polynomial function of degree $n-1$. In these functions, knots are the junction of the pieces. The B-spline is short for base spline, first introduced by Isaac Jacob Schoenberg. These basic functions are semi-orthogonal and have unique features that distinguish them for use in approximating functions. One of the most important features of B-spline functions is the continuity of themselves and their derivatives. An arbitrary function can be approximated by a linear combination of B-spline functions [14]. Linear B-spline functions (the second order) are as follows

$$\phi_{i,k}(t) = \begin{cases} t_i - k, & k \leq t_i < k+1, \\ 2-(t_i-k), & k+1\leq t_i < k+2, k = 0,\dots,2^i-2, \\ 0, & \text{otherwise}, \end{cases} \tag{4}$$

with left-hand side boundary functions

$$\phi_{i,k}(t) = \begin{cases} 2-(t_i-k), & 0 \le t_i < 1, k=-1, \\ 0, & \text{otherwise}, \end{cases} \tag{5}$$

and with right-hand side boundary functions

$$\phi_{i,k}(t) = \begin{cases} t_i-k, & k \le t_i < k+1, k=2^i-1, \\ 0, & \text{otherwise}. \end{cases} \tag{6}$$

The relation between t and t_i is $t_i = 2^i t$ [17].

2.3 Approximation by B-Spline Functions

To approximate an arbitrary function $f(t) \in L^2[0,1]$ through the B-spline functions, first let $i = M$ and then assume [18]

$$f(t) \simeq \sum_{k=-1}^{2^M-1} a_k \phi_{M,k}(t) = A^T \Phi_M(t), \tag{7}$$

where

$$\Phi_M = [\phi_{M,-1}(t), \phi_{M,0}(t), \ldots, \phi_{M,2^M-1}(t)]^T, \tag{8}$$

is a (2^M+1)-vector of the basis function similar to (4), (5) and (6) as follows

$$\phi_{M,-1}(t) = \begin{cases} 2-(2^M t+1), & 0 \le t < \frac{1}{2^M}, \\ 0, & \text{otherwise}, \end{cases} \tag{9}$$

$$\phi_{M,k}(t) = \begin{cases} 2^M t-k, & \frac{k}{2^M} \le t < \frac{k+1}{2^M}, \\ 2-(2^M t-k), & \frac{k+1}{2^M} \le t < \frac{k+2}{2^M}, \quad k=0,\ldots,2^M-2, \\ 0, & \text{otherwise}, \end{cases} \tag{10}$$

$$\phi_{M,2^M-1}(t) = \begin{cases} 2^M t-(2^M-1), & \frac{2^M-1}{2^M} < t \le 1, \\ 0, & \text{otherwise}, \end{cases} \tag{11}$$

and

$$A = [a_{-1}, a_0, \ldots, a_{2^M-1}]^T, \tag{12}$$

with

$$a_k = f(t_k), \quad t_k = \frac{k+1}{2^M}, \quad k=-1,\ldots,2^M-1, \tag{13}$$

where the points t_k are the collocation points [16, 17].

3 The Operational Matrix of Fractional Integration

This operational matrix was first obtained in [27] that we rewrite with some little changes. It is easy to see that the linear B-spline functions (9)-(11) can be written by

$$\phi_{M,-1}(t) = \left(1-2^M t\right)\left(\mu_0(t)-\mu_{\frac{1}{2^M}}(t)\right), \tag{14}$$

$$\phi_{M,k}(t) = \left(2^M t-k\right)\left(\mu_{\frac{k}{2^M}}(t)-\mu_{\frac{k+1}{2^M}}(t)\right) \tag{15}$$

$$+\left(2-2^M t+k\right)\left(\mu_{\frac{k+1}{2^M}}(t)-\mu_{\frac{k+2}{2^M}}(t)\right), \quad k=0,\dots,2^M-2, \tag{16}$$

$$\phi_{M,2^M-1}(t) = \left(2^M(t-1)+1\right)\left(\mu_{\frac{2^M-1}{2^M}}(t)-\mu_1(t)\right), \tag{17}$$

where $\mu_a(t)$ is the unit step function defined by

$$\mu_a(t) = \begin{cases} 1, & t \geq a, \\ 0, & t < a. \end{cases}$$

By taking the Laplace transform from Equations (14)-(17) we get

$$\mathscr{L}\{\phi_{M,-1}(t)\} = \frac{1}{s}\left(1+\frac{2^M}{s}\left(e^{-\frac{s}{2^M}-1}\right)\right), \tag{18}$$

$$\mathscr{L}\{\phi_{M,k}(t)\} = \frac{2^M}{s^2}\left(e^{-\frac{ks}{2^M}}-2e^{-\frac{(k+1)s}{2^M}}+e^{-\frac{(k+2)s}{2^M}}\right), \qquad k=0,1,\dots,2^M-2, \tag{19}$$

$$\mathscr{L}\{\phi_{M,2^M-1}(t)\} = \frac{2^M}{s^2}\left(e^{-\frac{(2^M-1)s}{2^M}}-e^{-s}\right)-\frac{e^{-s}}{s}. \tag{20}$$

According to Equation (2), the fractional integration of linear *B*-spline functions $\phi_{M,k}(t)$ of order α is

$$I^\alpha \phi_{M,k}(t) = \frac{1}{\Gamma(\alpha)}\left(t^{\alpha-1} * \phi_{M,k}(t)\right),$$

therefore, we have

$$\mathscr{L}\{I^\alpha \phi_{M,k}(t)\} = \frac{1}{s^\alpha}\mathscr{L}\{\phi_{M,k}(t)\}. \tag{21}$$

From Equations (18)-(20) and Equation (23), we get

$$\mathscr{L}\{I^\alpha \phi_{M,k}(t)\} = \frac{2^M}{s^{\alpha+2}}\begin{cases} \left(\frac{s}{2^M}-1\right)+e^{-\frac{s}{2^M}}, & k=-1, \\ e^{-\frac{ks}{2^M}}-2e^{-\frac{(k+1)s}{2^M}}+e^{-\frac{(k+2)s}{2^M}} & k=0,1,\dots,2^M-2, \\ e^{-\frac{(2^M-1)s}{2^M}}-\left(\frac{s}{2^M}+1\right)e^{-s}, & k=2^M-1. \end{cases} \tag{22}$$

Taking the inverse Laplace transform of Equation (22), we get

$$I^\alpha \phi_{M,k}(t) = \frac{2^M}{\Gamma(\alpha+2)}$$

$$\begin{cases} \left(t-\frac{1}{2^M}\right)^{\alpha+1}\mu_{\frac{1}{2^M}}(t)-\left(t-\frac{\alpha+1}{2^M}\right)t^{\alpha}, & k=-1,\\ \left(t-\frac{k}{2^M}\right)^{\alpha+1}\mu_{\frac{k}{2^M}}(t)-2\left(t-\frac{k+1}{2^M}\right)^{\alpha+1}\mu_{\frac{k+1}{2^M}}(t) & \\ +\left(t-\frac{k+2}{2^M}\right)^{\alpha+1}\mu_{\frac{k+2}{2^M}}(t), & k=0,1,\ldots,2^M-2,\\ \left(t-\frac{2^M-1}{2^M}\right)^{\alpha+1}\mu_{\frac{2^M-1}{2^M}}(t) & \\ -\left(t-1+\frac{\alpha+1}{2^M}\right)(t-1)^{\alpha}\mu_1(t), & k=2^M-1. \end{cases} \tag{23}$$

According to Equation (7), we expand $I^{\alpha}\Phi_{M,k}(t)$ by the linear B-spline functions as

$$I^{\alpha}\phi_{M,k}(t)\cong\sum_{i=-1}^{2^M-1}s_{ki}\phi_{M,k}(t)=\mathbf{S}_k^T\Phi_M(t), \tag{24}$$

where

$$s_{ki}=I^{\alpha}\phi_{M,k}\left(\frac{i+1}{2^M}\right) \qquad i,k=-1,\ldots,2^M-1, \tag{25}$$

S_k is a (2^M+1)-vector and Φ_M is the basis vector in Equation (8). Therefore, the operational matrix of fractional integration is obtained as follows

$$I^{\alpha}\Phi_M(t)\cong\mathcal{I}_{\alpha}\Phi_M(t). \tag{26}$$

Using Equations (23)-(25), it is easy to see that $\mathcal{I}_{\alpha}$ is a $(2^M+1)\times(2^M+1)$ matrix given by

$$\mathcal{I}_{\alpha}=\begin{bmatrix} 0 & \eta_0 & \eta_1 & \eta_2 & \cdots & \eta_{2^M-1}\\ & \kappa & \nu_1 & \nu_2 & \cdots & \nu_{2^M-1}\\ & & \kappa & \nu_1 & \cdots & \nu_{2^M-2}\\ & & & \ddots & \ddots & \vdots\\ & & & & \kappa & \nu_1\\ & & & & & \kappa \end{bmatrix}, \tag{27}$$

where $\kappa=\dfrac{1}{2^{M\alpha}\Gamma(\alpha+2)}$,

$$\eta_i=\kappa\Big[(\alpha-i)(i+1)^{\alpha}+i^{\alpha+1}\Big], \quad i=0,1,\ldots,2^M-1,$$

and

$$\nu_i=\kappa\Big[(i-1)^{\alpha+1}-2i^{\alpha+1}+(i+1)^{\alpha+1}\Big], \quad i=1,2,\ldots,2^M-1.$$

4 Problem Statement

This work aims to propose a new numerical method for approximating the solution of the following FOCP:

$$\text{Min(Max)}\ J(\mathbf{x},\mathbf{u}) = \int_0^1 \mathbf{L}(\mathbf{x}(t),\mathbf{u}(t),t)\,\mathrm{d}t, \tag{28}$$

$$s.t: \quad D^{\alpha}\mathbf{x}(t) = \mathbf{f}(\mathbf{x}(t),\mathbf{u}(t),t), \tag{29}$$

$$\mathbf{x}^{(k)}(0) = x_k, \qquad k = 0,1,\ldots,\lfloor\alpha\rfloor, \tag{30}$$

$$g_j(\mathbf{x}(t),D^{\alpha}\mathbf{x}(t),\mathbf{u}(t),t) \le 0, \quad j = 1,2,\ldots,w, \tag{31}$$

where $D^{\alpha} = [D^{\alpha_1}, D^{\alpha_2}, \ldots, D^{\alpha_l}]$ is the fractional derivative operator with

$$n_i - 1 < \alpha_i \le n_i, \quad n_i \in \mathbb{N}, \quad i = 1,2,\ldots,l,$$

and

$$\begin{aligned}\mathbf{x}(t) &= [x_1(t), x_2(t), \ldots, x_l(t)]^T,\\ \mathbf{u}(t) &= \left[u_1(t), u_2(t), \ldots, u_q(t)\right]^T,\\ \mathbf{f} &= [f_1, f_2, \ldots, f_l].\end{aligned}$$

Also, $\mathbf{L}$, f_i, and g_j, $i = 1,2,\ldots,l$, $j = 1,2,\ldots,w$ are linear or nonlinear functions. In addition, it should be noted that the elements of Equation (29) can be written as

$$D^{\alpha_i}x_i(t) = f_i(\mathbf{x}(t),\mathbf{u}(t),t), \qquad i = 1,2,\ldots,l. \tag{32}$$

5 The Proposed Numerical Method

In this section, we use the linear B-spline functions to solve FOCP as given in Equations (28)-(31). We expand $D^{\alpha_i}x_i(t)$ in Equation (32) by the linear B-spline functions as

$$D^{\alpha_i}x_i(t) \simeq \mathbf{Y}_i^T\Phi_M(t). \tag{33}$$

By using Equations (3), (26) and (33), we have

$$x_i(t) \simeq \mathbf{Y}_i^T\mathcal{I}_{\alpha_i}\Phi_M(t) + \sum_{k=0}^{n_i-1}\frac{t^k}{k!}x_i^{(k)}(0), \tag{34}$$

where $n_i - 1 < \alpha_i \leqslant n_i$. The expansion of the second term on the right-hand side of Equation (34) by the linear B-spline functions yields

$$x_i(t) \simeq \mathbf{Y}_i^T\mathcal{I}_{\alpha_i}\Phi_M(t) + \mathbf{A}_i^T\Phi_M(t) = \left(\mathbf{Y}_i^T\mathcal{I}_{\alpha_i} + \mathbf{A}_i^T\right)\Phi_M(t), \tag{35}$$

and by setting $\mathbf{X}_i^T = \mathbf{Y}_i^T\mathcal{I}_{\alpha_i} + \mathbf{A}_i^T$, we get

$$x_i(t) = \mathbf{X}_i^T\Phi_M(t). \tag{36}$$

For the control variables, we obtain

$$u_j(t) \simeq \mathbf{U}_j^T \Phi_M(t). \tag{37}$$

Let

$$\mathcal{I}_\alpha = \left[\mathcal{I}_{\alpha_1}, \mathcal{I}_{\alpha_2}, \dots, \mathcal{I}_{\alpha_l}\right],$$

and

$$\widehat{\Phi}_{M,l}(t) = I_l \otimes \Phi_M(t), \tag{38}$$

$$\widehat{\mathcal{I}_\alpha} = I_l \otimes \mathcal{I}_\alpha \tag{39}$$

$$\widehat{\Phi}_{M,q}(t) = I_q \otimes \Phi_M(t), \tag{40}$$

where I_l and I_q are identity matrices of order l and q respectively and $\otimes$ is the Kronecker product [19]. Now, by using Equations (38) and (40), we have

$$\mathbf{x}(t) \simeq \mathbf{X}^T \hat{\Phi}_{M,l}(t), \tag{41}$$

$$D^\alpha \mathbf{x}(t) \simeq \mathbf{Y}^T \hat{\Phi}_{M,l}(t), \tag{42}$$

$$\mathbf{u}(t) \simeq \mathbf{U}^T \hat{\Phi}_{M,q}(t), \tag{43}$$

where $\mathbf{X}$, $\mathbf{Y}$ and $\mathbf{A}$ are vectors of order $l(2^M+1)\times 1$, and $\mathbf{U}$ is a vector of order $q(2^M+1)\times 1$, given by

$$\mathbf{X} = \left[\mathbf{X}_1^T, \mathbf{X}_2^T, \dots, \mathbf{X}_l^T\right]^T,$$

$$\mathbf{Y} = \left[\mathbf{Y}_1^T, \mathbf{Y}_2^T, \dots, \mathbf{Y}_l^T\right]^T,$$

$$\mathbf{A} = \left[\mathbf{A}_1^T, \mathbf{A}_2^T, \dots, \mathbf{A}_l^T\right]^T,$$

$$\mathbf{U} = \left[\mathbf{U}_1^T, \mathbf{U}_2^T, \dots, \mathbf{U}_q^T\right]^T.$$

Moreover, by using Equation (39), we obtain $\mathbf{X} = \mathbf{Y}\widehat{\mathcal{I}_\alpha} + \mathbf{A}$. To approximate the objective function, we have two approaches, one related to when $\mathbf{L}(\mathbf{x}(t), \mathbf{u}(t), t)$ in (28) is quadratic as

$$\mathbf{L}(\mathbf{x}(t), \mathbf{u}(t), t) = \xi^T(t)\mathbf{Q}\xi(t) + \mathbf{u}^T(t)\mathbf{R}\mathbf{u}(t)$$

and we have

$$J(\mathbf{x}, \mathbf{u}) = \int_0^1 \left(\xi^T(t)\mathbf{Q}\xi(t) + \mathbf{u}^T(t)\mathbf{R}\mathbf{u}(t)\right) \mathrm{d}t, \tag{44}$$

then by substituting Equations (41) and (43) in Equation (44) we get

$$\begin{aligned} J(\mathbf{x}, \mathbf{u}) =& \mathbf{X}^T \left(\int_0^1 \widehat{\Phi}_{M,l}(t)\mathbf{Q}[\widehat{\Phi}_{M,l}(t)]^T \,\mathrm{d}t\right)\mathbf{X} \\ &+ \mathbf{U}^T \left(\int_0^1 \widehat{\Phi}_{M,q}(t)\mathbf{R}[\widehat{\Phi}_{M,q}(t)]^T \,\mathrm{d}t\right)\mathbf{U}. \end{aligned} \tag{45}$$

Equation (45) can be computed more efficiently by writing J as

$$J(\mathbf{x}, \mathbf{u}) = \mathbf{X}^T \left(\int_0^1 \mathbf{Q} \otimes \Phi_M(t)[\Phi_M(t)]^T \,\mathrm{d}t\right)\mathbf{X}$$

$$+\mathbf{U}^T\left(\int_0^1 \mathbf{R}\otimes\Phi_M(t)[\Phi_M(t)]^T\,\mathrm{d}t\right)\mathbf{U}. \tag{46}$$

Finally, $J(\mathbf{X},\mathbf{U})$ can be rewritten as

$$J(\mathbf{X},\mathbf{U}) = \mathbf{X}^T\left(\mathbf{Q}\otimes\mathbf{P}\right)\mathbf{X} + \mathbf{U}^T\left(\mathbf{R}\otimes\mathbf{P}\right)\mathbf{U}. \tag{47}$$

Otherwise, in the case that $\mathbf{L}(\mathbf{x}(t),\mathbf{u}(t),t)$ in (28) is an arbitrary function, we calculate it by a suitable Newton-Cotes numerical integration method [33] as

$$J(\mathbf{X},\mathbf{U}) = \sum_{i=0}^{n}\omega_i\mathbf{L}([\hat{\Phi}_{M,l}(t_i)]^T\mathbf{X},[\hat{\Phi}_{M,q}(t_i)]^T\mathbf{U},t_i), \quad t_i = \frac{i}{n}, i = 1,2,\ldots,n \tag{48}$$

where the weight ω_i is determined by

$$\omega_i = \int_0^1 l_i(t)\,\mathrm{d}t,$$

and each $l_i(t)$ is the Lagrange polynomial

$$l_i(t) = \prod_{\substack{j=0\\ j\neq i}}^{n}\frac{t-\tau_j}{\tau_i-\tau_j}.$$

Finally, we approximate the dynamic system as follows.
Using Equations (41)-(43) the system constraints (29) and (31) become

$$\mathbf{Y}^T\widehat{\Phi}_{M,l}(t) = \mathbf{f}(\mathbf{X}^T\widehat{\Phi}_{M,l}(t),\mathbf{U}^T\widehat{\Phi}_{M,q}(t),t), \tag{49}$$

$$\mathbf{g}_j([\hat{\Phi}_{M,l}(t)]^T\mathbf{X},[\hat{\Phi}_{M,q}(t)]^T\mathbf{U},t) \leqslant 0, \qquad j = 1,2,\ldots,w. \tag{50}$$

We collocate Equations (49) and (50) at

$$t_k = \frac{k-1}{2^M}, \quad k = 1,2,\ldots,2^M+1, \tag{51}$$

as

$$\mathbf{Y}^T\widehat{\Phi}_{M,l}(t_k) = \mathbf{f}(\mathbf{X}^T\widehat{\Phi}_{M,l}(t_k),\mathbf{U}^T\widehat{\Phi}_{M,q}(t_k),t_k), \tag{52}$$

$$\mathbf{g}_j([\hat{\Phi}_{M,l}(t_k)]^T\mathbf{X},[\hat{\Phi}_{M,q}(t_k)]^T\mathbf{U},t_k) \leqslant 0, \qquad j = 1,2,\ldots,w. \tag{53}$$

In this way, we were able to turn FOCP into a nonlinear programming problem which can be stated as follows. Find $\mathbf{X}$ and $\mathbf{U}$ so that $J(\mathbf{X},\mathbf{U})$ in Equations (47) or (48) is minimized (or maximized) subject to Equations (52) and (53). To solve this nonlinear programming problem, we use the NLPSolve command in Maple software, which uses the sequential quadratic programming (SQP) method to solve NLP.

6 Convergence of the Method

To check the convergence of the proposed numerical method, we first express the existence of the optimal solution in the form of Filippov's existence theorem. Suppose the usual set of augmented velocities defined by

$$(f, L_+)(x, U, t) := \{(f(x,u,t), L(x,u,t)+\gamma) | u \in U, \gamma \geq 0\} \subset \mathbb{R}^{n+1},$$

for all $(x,t) \in \mathbb{R}^n \times [0,1]$. Moreover let $\mathcal{T} \subset \mathcal{C}$ stand for the set of all trajectories x that can be associated with a control u such that the couple (x,u) satisfies all the constraints of the problem FOCP has given in Equations (28)-(31).

Theorem 1. (Filippov's existence theorem) Assume that U is compact, $\mathcal{T}$ is nonempty and bounded in C, and $(f, L_+)(x, U, t)$ is convex for all $(x,t) \in \mathbb{R}^n \times [0,1]$. Then problem FOCP given in Equations (28)-(31) has at least one optimal solution.

Proof. Refer to [5]. □

Now we know that FOCP given in Equations (28)-(31) has at least one optimal solution of the form (x^*, u^*). So, to show that the method is convergent, it is sufficient $\|x - x^*\| \to 0$ and $\|u - u^*\| \to 0$ as $M \to \infty$ where x and u are approximate values obtained from the proposed numerical method and M is the parameter of the method related to the collocation points. We consider a linear B-spline space $\mathbb{S}_{M,\boldsymbol{\tau}} = \text{span}\{\phi_{M,-1}, \phi_{M,0}, \ldots, \phi_{M,2^M-1}\}$ where $\phi_{M,k}$, $k = -1, 0, \ldots, 2^M - 1$ are *B*-spline functions defined in Equations (4-6) also $\boldsymbol{\tau} = (\tau_j)_{j=1}^{2^M+1}$ where $\tau_j = \frac{j-1}{2^M}$. Assuming that $h_j = \tau_{j+1} - \tau_j$ and $h = \max_{j=1,\ldots,2^M+1} h_j$, we have $h = \frac{1}{2^M}$. For an arbitrary function f we consider the distance from f to $\mathbb{S}_{2,\tau}$ defined by

$$\text{dist}_{\infty,[0,1]}(f, \mathbb{S}_{M,\boldsymbol{\tau}}) = \inf_{g \in \mathbb{S}_{M,\tau}} \|f - g\|_{\infty,[0,1]}.$$

Theorem 2. Suppose that an arbitrary function $f \in C^3[0,1]$ is given. Then for the linear B-spline space $\mathbb{S}_{M,\boldsymbol{\tau}}$

$$\text{dist}_{\infty,[0,1]}(f, \mathbb{S}_{2,\boldsymbol{\tau}}) \leq K h^3 \|D^3 f\|_{\infty,[0,1]},$$

where $K = \frac{1}{2^3 3!}$ and $D^3 f$ is the third derivative of the function f.

Proof. Refer to [22]. □

Now, according to $h = \frac{1}{2^M}$, by increasing the value of M sufficiently, we can bring the values of the state and control variables closer to their optimal values.

7 Illustrative Examples

In this section, by solving numerical examples, we will clarify the steps of using the proposed numerical method. We used the Maple 2015 program on a personal computer to perform numerical calculations

Example 1. We consider the following time-invariant FOCP from [2]

$$\min J = \frac{1}{2}\int_0^1 [x^2(t) + u^2(t)]\,\mathrm{d}t, \tag{54}$$

subject to the system dynamics

$$D^\alpha x(t) = -x(t) + u(t), \tag{55}$$

and the initial condition

$$x(0) = 1. \tag{56}$$

The exact solution to this problem in the case $\alpha = 1$ is

$$\begin{aligned}
\bar{x}(t) &= \cosh(\sqrt{2}t) + \beta \sinh(\sqrt{2}t),\\
\bar{u}(t) &= (1 + \sqrt{2}\beta)\cosh(\sqrt{2}t) + (\sqrt{2} + \beta)\sinh(\sqrt{2}t),
\end{aligned}$$

where

$$\beta = -\frac{\cosh(\sqrt{2}) + \sqrt{2}\sinh(\sqrt{2})}{\sqrt{2}\cosh(\sqrt{2}) + \sinh(\sqrt{2})} \simeq -0.979921727.$$

The optimal value of the performance index with the exact solution is $J = 0.1929093$. Assume that $\widetilde{x}(t)$, $\widetilde{u}(t)$ and $\widetilde{J}(x,u)$ are the approximate values obtained from numerical methods for the state, control, and objective functions respectively. Then the error is given by

$$\begin{aligned}
E_x &= \max_i(|\bar{x}(t_i) - \widetilde{x}(t_i)|),\\
E_u &= \max_i(|\bar{u}(t_i) - \widetilde{u}(t_i)|),\\
E_J &= |\bar{J} - \widetilde{J}|,
\end{aligned}$$

where $t_i = \frac{i+1}{2^M}$, $i = -1, \ldots, 2^M - 1$. Figure 1 demonstrates state and control variables obtained by our numerical method for $M = 8$ and different values of α. Figure 2 shows the logarithmic graphs of MAEs (Maximum Absolute Errors) of $x(t)$, $u(t)$ and J for $\alpha = 1$ and different values of M. Given these figures, the convergence of the method can be deduced. Tables 1 and 2 show the absolute errors of the approximate optimal state $\widetilde{x}(t)$ and the absolute error of the optimal control $\widetilde{u}(t)$ respectively. Table 3 shows the approximate value of the performance index $\widetilde{J}$ and its error with the exact value of $\bar{J}$.

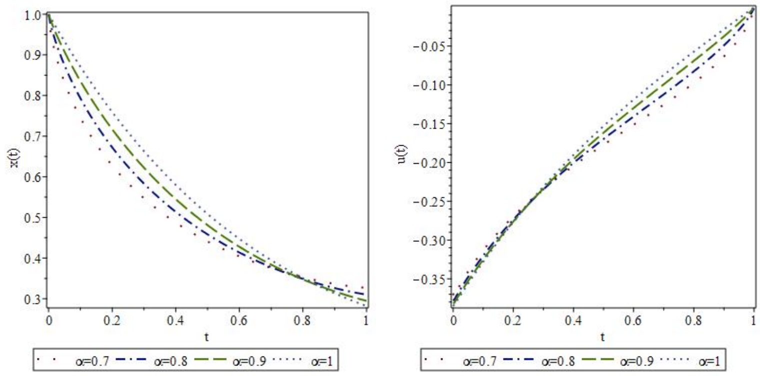

Figure 1: State $x(t)$ and control $u(t)$ functions for Example 1.

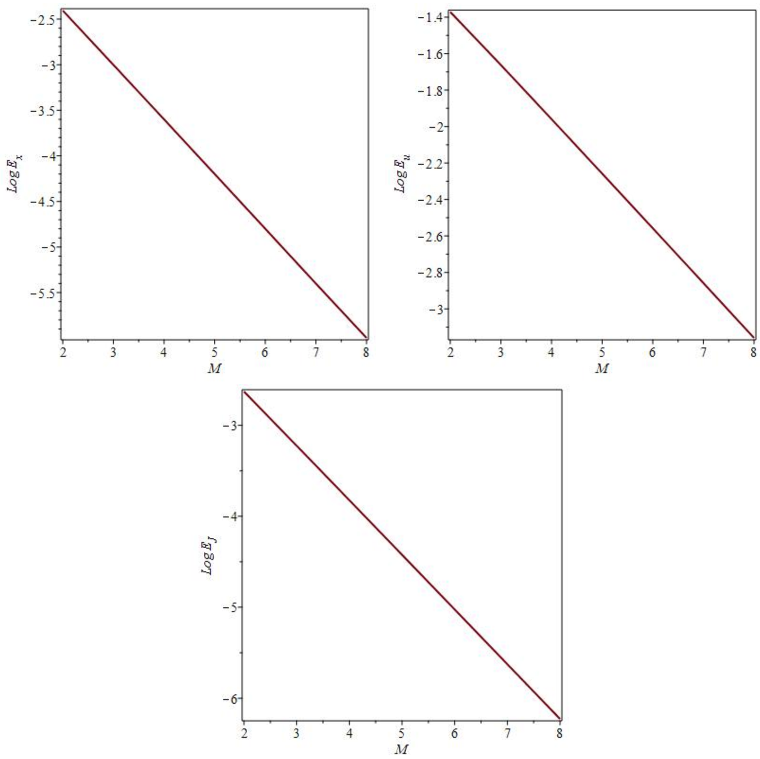

Figure 2: Logarithmic graphs of MAEs for Example 1.

Table 1: The absolute errors of the approximate optimal states for Example 1

t	Method of [15] for $N=5$	Method of [35] for $N=5$	Method of [13] for $M=8$	Presented method for $M=8$
0.1	2.11×10^{-5}	6.90×10^{-7}	1.44×10^{-6}	3.52×10^{-6}
0.2	9.71×10^{-6}	3.62×10^{-6}	1.36×10^{-6}	1.86×10^{-6}
0.3	4.08×10^{-7}	1.97×10^{-6}	1.23×10^{-6}	1.40×10^{-6}
0.4	5.76×10^{-7}	2.58×10^{-6}	1.01×10^{-6}	1.74×10^{-6}
0.5	5.66×10^{-6}	4.46×10^{-6}	2.92×10^{-7}	4.89×10^{-7}
0.6	9.25×10^{-6}	1.65×10^{-6}	7.79×10^{-7}	1.08×10^{-6}
0.7	8.35×10^{-6}	2.80×10^{-6}	7.85×10^{-7}	3.67×10^{-7}
0.8	4.36×10^{-6}	3.49×10^{-6}	6.71×10^{-7}	2.44×10^{-7}
0.9	2.59×10^{-6}	1.22×10^{-6}	5.32×10^{-7}	5.24×10^{-7}

Table 2: The absolute errors of the approximate optimal controls for Example 1

t	Method of [35] for $N=5$	Method of [15] for $N=5$	Method of [13] for $M=9$	Presented method for $M=9$
0.1	1.90×10^{-5}	6.74×10^{-6}	1.26×10^{-6}	1.56×10^{-6}
0.2	5.01×10^{-6}	3.17×10^{-6}	4.68×10^{-6}	7.33×10^{-7}
0.3	1.46×10^{-5}	5.92×10^{-7}	4.49×10^{-6}	4.37×10^{-7}
0.4	1.47×10^{-5}	7.10×10^{-7}	1.23×10^{-6}	4.51×10^{-7}
0.5	1.25×10^{-6}	2.01×10^{-6}	7.31×10^{-6}	3.20×10^{-7}
0.6	1.07×10^{-5}	2.71×10^{-6}	1.19×10^{-6}	7.20×10^{-8}
0.7	1.27×10^{-5}	2.11×10^{-6}	3.83×10^{-6}	1.57×10^{-7}
0.8	7.62×10^{-6}	8.59×10^{-7}	3.68×10^{-6}	1.74×10^{-7}
0.9	1.74×10^{-5}	8.93×10^{-8}	1.15×10^{-6}	5.36×10^{-8}

Table 3: The approximate values and their errors with exact values of $\bar{J}$ for Example 1

Method of [35]			Presented method		
N	$\bar{J}$	$E_J=\lvert\bar{J}-\widetilde{J}\rvert$	M	$\bar{J}$	$E_J=\lvert\bar{J}-\widetilde{J}\rvert$
2	0.1926605504081	2.48×10^{-4}	5	0.192909340640602	4.25×10^{-8}
3	0.1929127052722	3.41×10^{-6}	6	0.192909300753628	2.66×10^{-9}
4	0.1929092715551	2.65×10^{-8}	7	0.192909298259509	1.66×10^{-10}
5	0.1929092982262	1.33×10^{-10}	8	0.192909298103643	1.04×10^{-11}
6	0.1929092980936	6.15×10^{-13}	9	0.192909298093859	6.59×10^{-13}

Example 2. Consider the following fractional optimal control problem that was introduced in [21] and also was studied in [6]

$$\text{Min } J=\int_0^1\left[\left(x(t)-t^2\right)^2+\left(u(t)+t^4-\frac{20t^{\frac{9}{10}}}{9\Gamma(\frac{9}{10})}\right)^2\right]dt,$$

subject to the dynamic constraints

$$D^{1.1}x(t) = t^2 x(t) + u(t),$$
$$x(0) = \dot{x}(0) = 0.$$

The exact solution to this problem is given by

$$\bar{x}(t) = t^2,$$
$$\bar{u}(t) = \frac{20t^{\frac{9}{10}}}{9\Gamma(\frac{9}{10})} - t^4,$$
$$\bar{J} = 0.$$

The exact and approximate values of the state and control variables are illustrated in Figure 3, and their errors are plotted in Figure 4. The logarithmic graphs of MAEs of state and control variables and performance index are shown in Figure 5. In Table 4, the approximate values of the performance index J for different values of M, are presented. Also, these values are compared with similar methods in [6, 21]. According to Table 4, the presented method is more accurate than the existing methods.

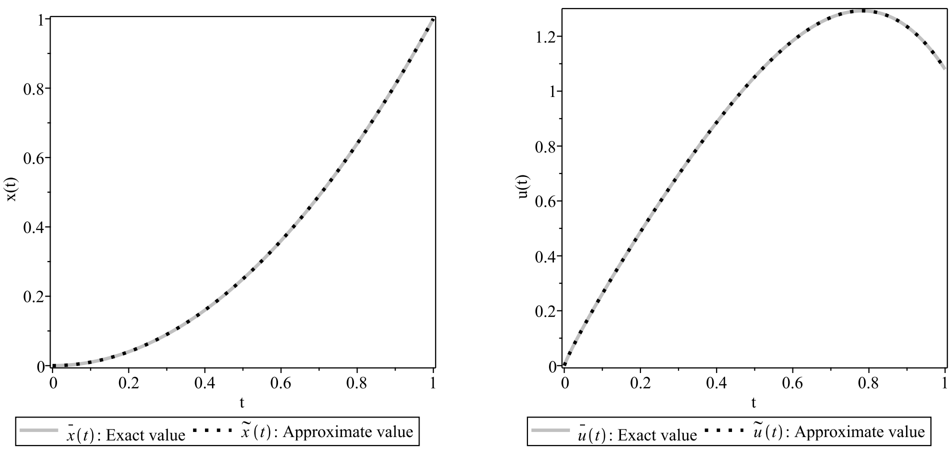

Figure 3: The values of $x(t)$ and $u(t)$ obtained by $M = 8$ for Example 2.

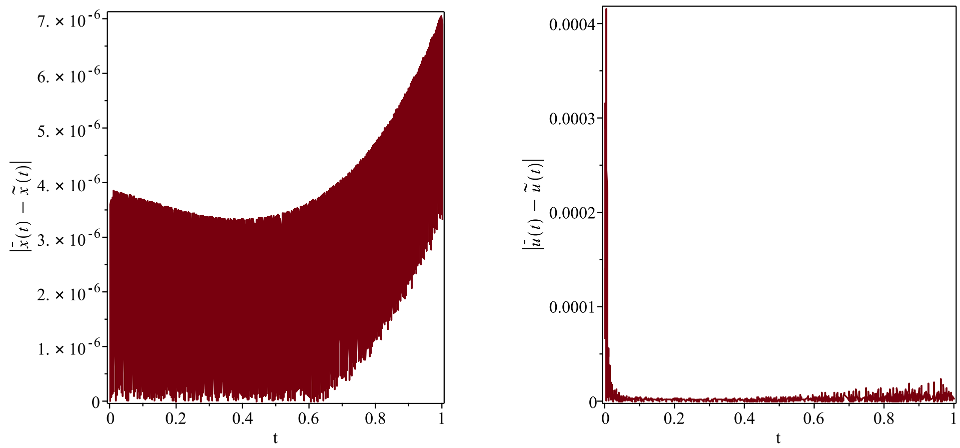

Figure 4: The values of errors of $x(t)$ and $u(t)$ obtained by $M = 8$ for Example 2.

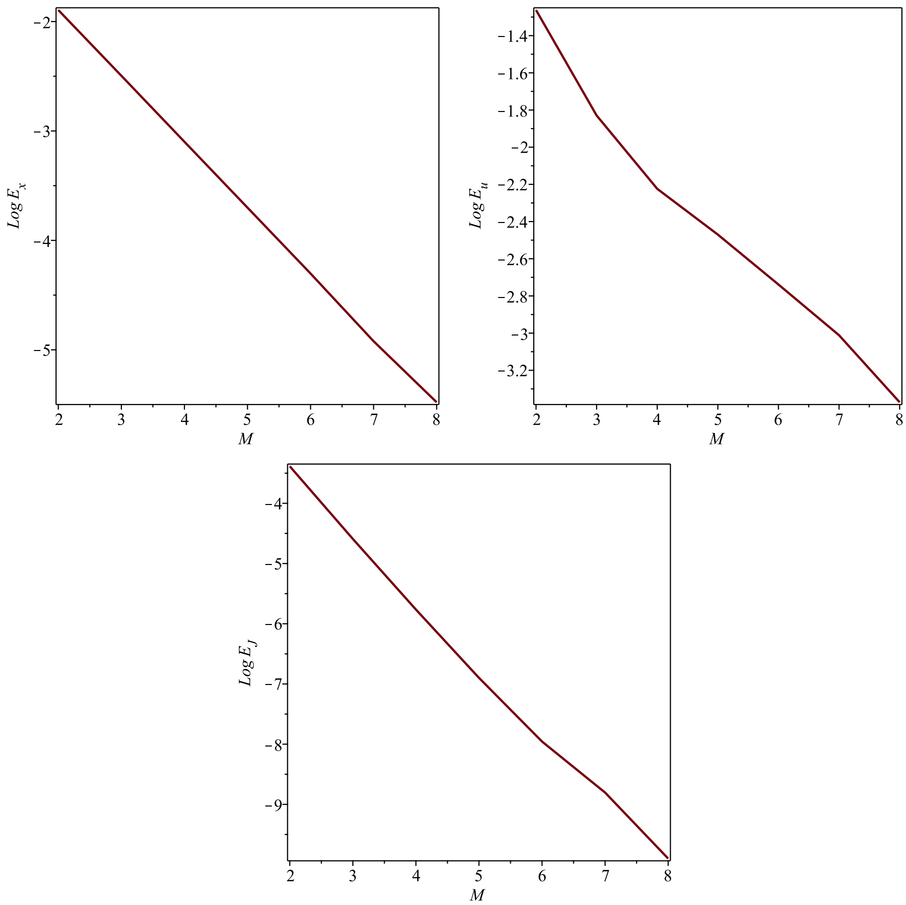

Figure 5: Logarithmic graphs of MAEs for Example 2.

Table 4: Approximate values of J for Example 2

Methods	Parameters of method	$J(x,u)$
Method of [21]	$(m=3, n=4)$	6.0753×10^{-6}
	$(m=4, n=5)$	1.67255×10^{-6}
	$(m=5, n=6)$	5.91532×10^{-7}
	$(m=7, n=8)$	1.21966×10^{-7}
	$(m=8, n=9)$	7.03371×10^{-8}
Method of [6]	$N=4$	4.76932×10^{-6}
	$N=5$	1.47243×10^{-6}
	$N=6$	5.37825×10^{-7}
	$N=8$	1.06099×10^{-7}
	$N=9$	5.44304×10^{-8}
The present method	$M=4$	$1.72145571012670767\times10^{-6}$
	$M=5$	$1.26295831601775329\times10^{-7}$
	$M=6$	$1.10567794682908139\times10^{-8}$
	$M=7$	$1.57143831079185382\times10^{-9}$
	$M=8$	$1.26073358425454064\times10^{-10}$

Example 3. Consider the following FOCP [21]

$$\begin{aligned}\text{Min } J = \int_0^1 \Bigg[&\exp(t)\left(x(t) - t^4 + t - 1\right)^2 \\ &+ \left(1+t^2\right)\left(u(t) + 1 - t + t^4 - \frac{8000 t^{\frac{21}{10}}}{77\Gamma\left(\frac{1}{10}\right)}\right)^2\Bigg] \mathrm{d}t,\end{aligned}$$

subject to the dynamic system

$$D^{1.9}x(t) = x(t) + u(t), \qquad t \in [0,1],$$

and the boundary conditions

$$x(0) = 1, \quad \dot{x}(0) = -1.$$

The exact solution is given by

$$\begin{aligned}\bar{x} &= 1 - t + t^4, \\ \bar{J} &= 0.\end{aligned}$$

In Figure 6, the exact and approximate values of the state variable and approximate value of the control variable with $M = 8$ are illustrated. Moreover, we plotted the error value of $x(t)$ in Figure 7. The MAEs of state vector $x(t)$ and performance index J are plotted in Figure 8.

Example 4. In this example, we present a problem involving a two-dimensional state variable and an inequality constraint

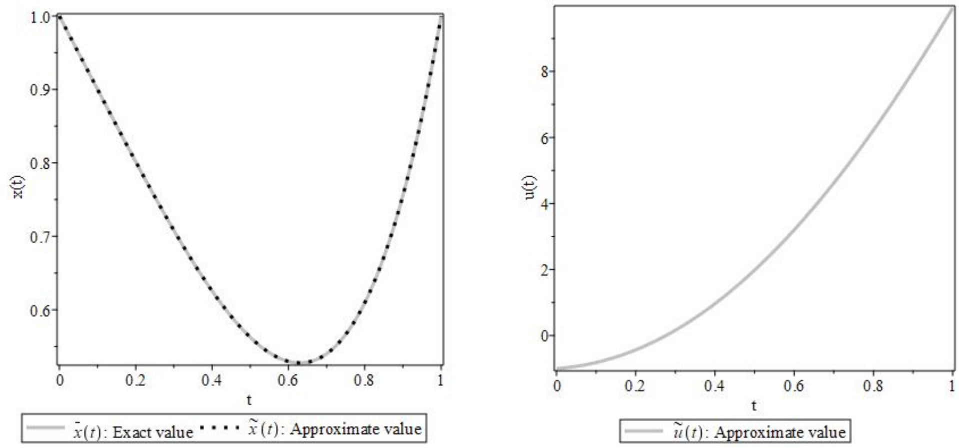

Figure 6: The values of $x(t)$ and $u(t)$ obtained by $M = 8$ for Example 3.

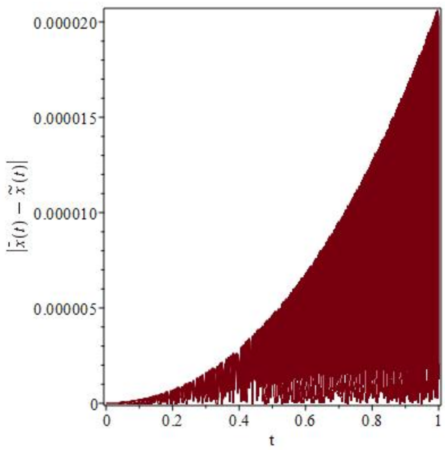

Figure 7: The values of errors of $x(t)$ obtained by $M = 8$ for Example 3.

$$\min J = \frac{1}{2}\int_0^1 u^2(t)\,\mathrm{d}\,t,$$

subject to

$$\begin{aligned}
&\mathrm{D}^{\alpha}\,x_1(t) = x_2(t),\\
&\mathrm{D}^{\alpha}\,x_2(t) = u(t),\\
&x_1(t) \le 0.1,\\
&x_1(0) = x_1(1) = 0,\\
&x_2(0) = -x_2(1) = 1.
\end{aligned}$$

The exact values of the control variable for $\alpha = 1$ are

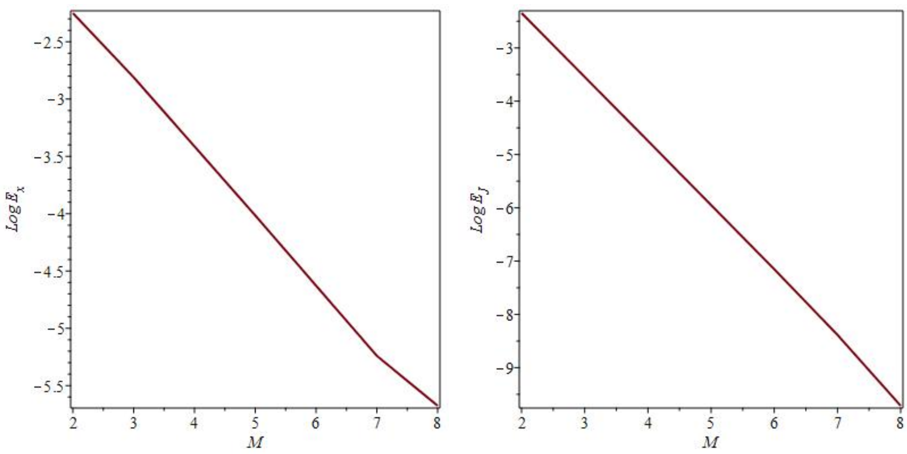

Figure 8: Logarithmic graphs of MAEs for Example 3.

Table 5: Approximate values of J for Example 3

Methods	Parameters of the method	$J(x,u)$
The method of [21]	$m=n=3$	8.93768×10^{-6}
	$m=n=4$	5.42028×10^{-7}
	$m=n=5$	6.77757×10^{-8}
	$m=n=7$	2.84624×10^{-9}
	$m=n=8$	8.22283×10^{-10}
The present method	$M=4$	$1.80165706993258757\times10^{-5}$
	$M=5$	$1.12585635458861543\times10^{-6}$
	$M=6$	$7.02177422426594986\times10^{-8}$
	$M=7$	$4.12444733804727959\times10^{-9}$
	$M=8$	$1.92637108047034916\times10^{-10}$

$$u^*(t)=\begin{cases}\frac{200}{9}t-\frac{20}{3}, & t\in[0,0.3],\\ 0, & t\in[0.3,0.7],\\ -\frac{200}{9}t+\frac{140}{9} & t\in[0.7,1].\end{cases}$$

Figure 9 shows the exact and approximate states and control variables obtained by the proposed method for $M=8$ and $\alpha=1$.

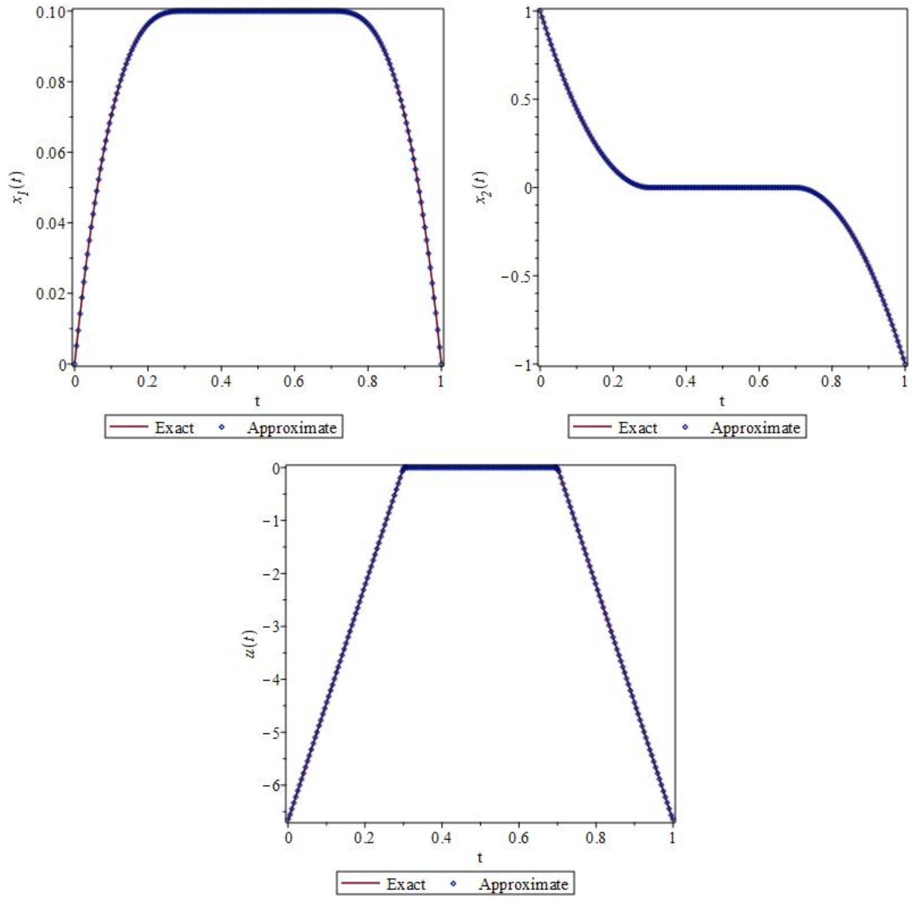

Figure 9: State functions $x_1(t)$ and $x_2(t)$ and control function $u(t)$ for Example 4.

8 Conclusion

In this paper, we presented a numerical method with an emphasis on better accuracy than similar tasks. In this method, we used B-spline functions, and the distinguishing feature of this work is the use of a fractional integral operational matrix in solving the FOCPs. We managed to turn FOCP into NLP with the help of this matrix. Using several numerical examples, we were able to show the high efficiency, and accuracy of the proposed method. In addition, by increasing the value of M, the accuracy of the method increases, and in cases where there is an exact solution, the approximate value converges to the exact solution, and also the error is reduced. For future research, more accurate approximations can be achieved by extending the basic functions for approximation.

References

[1] Adams M. P. (2018). "Numerical schemes for the fractional calculus and their application to image feature detection", (Master's thesis, Graduate Studies).

[2] Agrawal O. P. (1989). "General formulation for the numerical solution of optimal control problems", International Journal of Control, 50, 627-638.

[3] Baghani O. (2021). "Second Chebyshev wavelets (SCWs) method for solving finite-time fractional linear quadratic optimal control problems", Mathematics and Computers in Simulation, 190, 343-361.

[4] Baghani O. (2022). "SCW-iterative-computational method for solving a wide class of nonlinear fractional optimal control problems with Caputo derivatives", Mathematics and Computers in Simulation, 202, 540-558.

[5] Bergounioux M., Bourdin L. (2020). "Pontryagin maximum principle for general Caputo fractional optimal control problems with Bolza cost and terminal constraints", ESAIM: Control, Optimisation and Calculus of Variations, 26, 35.

[6] Bhrawy A. H., Doha E. H., Baleanu D., Ezz-eldien S. S., Abdelkawy M. A. (2015). "An accurate numerical technique for solving fractional optimal control problems", Differential Equations, 15, 23.

[7] Darehmiraki M. (2018). "An efficient solution for stochastic fractional partial differential equations with additive noise by a meshless method", International Journal of Applied and Computational Mathematics, 4, 14.

[8] Das S. (2011). "Functional fractional calculus", Springer-Verlag Berlin Heidelberg.

[9] Doha E. H., Bhrawy A. H., Baleanu D., Ezz-Eldien S. S., Hafez R. M. (2015). "An efficient numerical scheme based on the shifted orthonormal Jacobi polynomials for solving fractional optimal control problems", Advances in Difference Equations, 15.

[10] Edrisi Tabriz Y., Heydari A. (2014). "Generalized B-spline functions method for solving optimal control problems", Computational Methods for Differential Equations, 2, 243-255.

[11] Edrisi Tabriz Y., Lakestani M. (2015) "Direct solution of nonlinear constrained quadratic optimal control problems using B-spline functions", Kybernetika, 51, 81-98.

[12] Edrisi Tabriz Y., Lakestani M., Heydari A. (2016). "Two numerical methods for nonlinear constrained quadratic optimal control problems using linear B-spline functions", Iranian Journal of Numerical Analysis and Optimization, 6, 17-38.

[13] Edrisi-Tabriz Y., Lakestani M., Razzaghi M. (2021). "Study of B-spline collocation method for solving fractional optimal control problems", Transactions of the Institute of Measurement and Control, 43(11), 2425-37.

[14] Goswami J. C., Chan A. K. (2011). "Fundamentals of wavelets: theory, algorithms, and applications", John Wiley & Sons.

[15] Habibli M., Noori Skandari M. H. (2019). "Fractional Chebyshev pseudo spectral method for fractional optimal control problems", Optimal Control Applications and Methods, 40(3), 558-572.

[16] Lakestani M., Razzaghi M., Dehghan M. (2006). "Semiorthogonal spline wavelets approximation for Fredholm integro-differential equations", Mathematical Problems in Engineering.

[17] Lakestani M., Razzaghi M., Dehghan M. (2005). “Solution of nonlinear Fredholm-Hammerstein integral equations by using semiorthogonal spline wavelets”, Mathematical Problems in Engineering, 113-121.

[18] Lakestani M., Dehghan M., Irandoust-Pakchin S. (2012). “The construction of operational matrix of fractional derivatives using B-spline functions”, Communications in Nonlinear Science and Numerical Simulation, 17, 1149-1162.

[19] Lancaster P., Tismenetsky M. (1985). “The theory of matrices: with applications”, Elsevier.

[20] Laskin N. (2018). “Fractional quantum mechanics”, World Scientific.

[21] Lotfi A., Yousefi S. A., Dehghan M. (2013). “Numerical solution of a class of fractional optimal control problems via the Legendre orthonormal basis combined with the operational matrix and the Gauss quadrature rule”, Journal of Computational and Applied Mathematics, 250, 143-160.

[22] Lyche T., Morken K. (2008). “Spline methods draft”, Department of Informatics, Center of Mathematics for Applications, University of Oslo, Oslo, 3-8.

[23] Magin R., Vinagre B., Podlubny I. (2018). “Can cybernetics and fractional calculus be partners?: Searching for new ways to solve complex problems”, IEEE Systems, Man, and Cybernetics Magazine, 4(3), 23-28.

[24] Nemati A., Yousefi S., Soltanian F., Ardabili J. S. (2016). “An efficient numerical solution of fractional optimal control problems by using the Ritz method and Bernstein operational matrix”, Asian Journal of Control, 18, 2272-2282.

[25] Rabiei K., Ordokhani Y., Babolian E. (2016). “The Boubaker polynomials and their application to solve fractional optimal control problems”, Nonlinear Dynamic, 88, 1013-1026.

[26] Rao A. V. (2009). “A survey of numerical methods for optimal control”, Advances in the Astronautical Sciences, 135, 497-528.

[27] Saeedi H. (2017). “The linear b-spline scaling function operational matrix of fractional integration and its applications in solving fractional-order differential equations”, Iranian Journal of Science and Technology, Transaction A, 41, 723-733.

[28] Schoenberg I. J. (1973). “Cardinal spline interpolation”, Society for Industrial and Applied Mathematics.

[29] Schoenberg I. J. (1946). “Contributions to the problem of approximation of equidistant data by analytic functions Part B. On the problem of osculatory interpolation. A second class of analytic approximation formulae”, Quarterly of Applied Mathematics, 4(2), 112-141.

[30] Shukla M. K., Sharma B. B., Azar A. T. (2018). “Control and synchronization of a fractional order hyperchaotic system via backstepping and active backstepping approach”, In Mathematical Techniques of Fractional Order Systems, Elsevier, 559-595.

[31] Skandari M. H. N., Habibli M., Nazemi A. (2020). “A direct method based on the Clenshaw-Curtis formula for fractional optimal control problems”, Mathematical Control & Related Fields, 10(1), 171.

[32] Sopasakis P., Sarimveis H., Macheras P., Dokoumetzidis A. (2018). “Fractional calculus in pharmacokinetics”, Journal of pharmacokinetics and pharmacodynamics, 45(1), 107-125.

[33] Stoer J., Bulirsch R. (2013). “Introduction to numerical analysis”, Springer Science & Business Media.

[34] Unser M., Blu T. (2000). “Fractional Splines and Wavelets”, SIAM Review, 42, 43-67.

[35] Xiaobing P., Yang X., Skandari M. H. N., Tohidi E., Shateyi S. (2022). “”A new high accurate approximate approach to solve optimal control problems of fractional order via efficient basis functions”, Alexandria Engineering Journal, 61(8), 5805-5818.

[36] Yaghi M., Efe M. Ö. (2018). “Fractional order PID control of a radar guided missile under disturbances”, In: Information and Communication Systems (ICICS), 2018 9th International Conference, 238-242.

[37] Yang Y., Noori Skandari M. H. (2020). “Pseudo spectral method for fractional infinite horizon optimal control problems”, Optimal Control Applications and Methods, 41(6), 2201-2212.

[38] Yang X., Yang Y., Skandari M. N., Tohidi E., Shateyi S. (2022). “A new local non-integer derivative and its application to optimal control problems”, AIMS Mathematics, 7(9), 16692-16705.

[39] Yonthanthum W., Rattana A., Razzaghi M. (2018). “An approximate method for solving fractional optimal control problems by the hybrid of block-pulse functions and Taylor polynomials”, Optimal Control Applications and Methods, 39, 873-887.

How to Cite this Article:

Edrisi-Tabriz, Y. (2022). “Using the Integral Operational Matrix of *B*-Spline Functions to Solve Fractional Optimal Control Problems”, Control and Optimization in Applied Mathematics, 7(2): 77-98. doi: 10.30473/coam.2022.62261.1207